Ref.TH.2220-CERN

W BOSON PRODUCTION IN e^+e^- COLLISIONS IN THE WEINBERG - SALAM MODEL

W. Allès

Istituto di Fisica dell ' Università, Bologna
Istituto Nazionale di Fisica Nucleare,
Sezione di Bologna

Ch. Boyer

Laboratoire de Physique Théorique
et Particules Elémentaires *), Orsay

and

A.J. Buras

CERN -- Geneva

A B S T R A C T

We study W boson production in e^+e^- collisions in the Weinberg-Salam model. We first estimate Z^o contribution to the process $e^+e^- \to W^-e^+\nu$. It turns out that this contribution in spite of the enhancement through Z^o propagator gives $\sigma \sim 10^{-38}$ cm^2 and is as small as other contributions to this process, discussed by other authors. We conclude that $e^+e^- \to W^-e^+\nu$ is not a good place to look for W's and study next the process $e^+e^- \to W^-W^+$ which in spite of its higher threshold is more suitable for W search giving $\sigma \sim 10^{-35}$ cm^2. We present explicit formulae and corresponding numerical estimates of the total cross-sections and angular distributions for $e^+e^- \to W^+W^-$. We also calculate the separate contributions to the latter process coming from various diagrams and their interference terms and conclude that strong cancellations between various contributions should be expected already just above the threshold for the process in question.

---

*) Laboratoire associé au C.N.R.S.

Ref.TH.2220-CERN

1 September 1976

1. - INTRODUCTION

The attempts of gauge theorists to construct renormalizable unified models of weak and electromagnetic interactions of hadrons and leptons led some time ago to the incorporation of many new objects into the world of elementary particles. Among others the most prominent ones are

i) new gauge bosons (brothers of the photon), as for instance Z^0 (responsible for weak neutral current induced processes) and $W^{\pm}$ (responsible for charged current induced processes) in the Weinberg-Salam (WS) model [1] ;

ii) heavy leptons, which are used in many gauge models to make them consistent with unitarity [2] ;

iii) Higgs bosons, needed to give masses to the gauge bosons as well as to elementary fermions ; and

iv) charmed particles, needed to suppress strangeness changing neutral currents [3].

The experimental discoveries of the last few years seem to indicate that at least some of the above mentioned particles are not just theoretical inventions, but truly existing objects.

In fact neutral currents (and thus indirectly neutral vector bosons) [4], ψ/J family (presumably bound states of charm-anticharm quarks) [5] as well as charmed mesons ($\mathcal{D}^0, \mathcal{D}^{\pm}$) [6] have been seen. There is also a good indication that a new heavy lepton may exist [7].

All these findings make us believe that gauge theories are very strong candidates for being the correct description of weak and electromagnetic interactions. Clearly in order to prove the correctness of these theories, further findings are necessary, as for instance discovery of Z^0, $W^{\pm}$ and Higgs bosons. A very detailed discussion of the phenomenology of the Higgs bosons has been presented in Ref. 8). Also estimates of the production of $W^{\pm}$ and Z^0 in pp and deep inelastic neutrino processes have been made [9].

As regards e^+e^- collisions, they should be obviously useful for Z^o production. On the other hand, less is known about the W production in the collisions in question. To our best knowledge there exist in the literature only estimates of the total cross-section for $e^+e^- \rightarrow W^+W^-$ [10)-12)] and calculations of some contributions to the process $e^+e^- \rightarrow W^-e^+\nu$ [13)]. In particular, it seems that the estimate of the Z^o contribution to the latter process (See Fig. 1, diagrams b and c) is missing in the literature. This contribution could be important due to enhancement through the Z propagator. Since the process $e^+e^- \rightarrow W^-e^+\nu$, having smaller threshold than the process $e^+e^- \rightarrow W^+W^-$, is preferred from the budget point of view, it is of interest to estimate its cross-section with the Z^o contribution included. This we do in Section 3 in the framework of the Weinberg-Salam model. It turns out that $\sigma(e^+e^- \rightarrow W^-e^+\nu) \sim O(10^{-38}\ cm^2)$ and consequently the process in question is not very useful for W production. Therefore, in Section 4 we make a detailed study of the process $e^+e^- \rightarrow W^+W^-$ which, for energies $130 \leq \sqrt{s} \leq 180$ GeV, has cross-section $\sigma \sim O(10^{-35}\ cm^2)$ in the Weinberg-Salam model, and is experimentally feasible. We first present explicit formulae for total cross-section and angular distributions and then discuss the corresponding numerical estimates.

Our results for the total cross-section $\sigma(e^+e^- \rightarrow W^+W^-)$ agree with those obtained in Ref. 11). These authors, however, did not present estimates of the angular distributions nor did they give explicit formulae for separate contributions of various diagrams.

As already stated, our calculations are in the framework of the Weinberg-Salam model. The reason for choosing this particular model is that it is the simplest gauge model consistent with data. It has only one free parameter (if we neglect lepton masses and consequently the couplings to Higgs particles), the mixing angle θ_W which is "known" from the fits of the W-S model to various processes to be in the range $0.25 < \sin^2\theta < 0.5$, the canonical value being $\sin^2\theta = 3/8 \approx 0.37$ *). Thus in the framework of the model in question, definite numerical predictions can be made.

---

*) This is the value predicted by a class of grand unifying schemes for strong, weak and electromagnetic interactions. See, for instance, Ref. 14).

Our interest in the calculation of the cross-sections for $e^+e^- \to W^+W^-$ is two-fold. First as already mentioned we are interested in experimental predictions. Second, the process $e^+e^- \to W^+W^-$ is of interest to us since it is one of those processes which, in pre-gauge theories (with only γ and ν contributions included, see Fig. 2) led to violation of unitarity. It is well known that this bad behaviour can be cured by adding the diagram b) of Fig. 2 involving Z^0 and choosing Yang-Mills couplings [15]. Thus it is of interest to investigate at which energy the required cancellation of badly behaving terms starts to be effective or, equivalently, at which energy the Z^0 starts to play an important rôle.

The paper is organized as follows. In Section 2 we recall the Feynman rules for the W-S model, as well as relations between parameters of the model. In Section 3 the process $e^+e^- \to W^-e^+\nu$ is discussed. In Section 4, explicit formulae for $\sigma(e^+e^- \to W^+W^-)$ and $(d\sigma/d\Omega)(e^+e^- \to W^+W^-)$ together with corresponding numerical estimates are given. Section 5 contains a summary and the conclusions.

2. - FEYNMAN RULES AND PARAMETERS OF THE WEINBERG-SALAM MODEL

In this section we recall the Feynman rules which we have used in our calculations. We work in the unitary gauge. Our conventions are those of Ref. 16).

The Feynman rules in the W-S model are summarized in Fig. 3. The relations between various couplings and parameters appearing there are as follows

$$a = \frac{1}{4} - \sin^2\Theta_W \quad , \quad b = \frac{1}{4} \quad ,$$

$$G = -\frac{2e}{\sin 2\Theta_W} \quad , \quad Z = e \operatorname{ctg} \Theta_W$$

$$\tilde{g} = -\frac{e}{\sqrt{2}\, 2 \sin\Theta_W} \quad , \quad M_Z = \frac{M}{\cos\Theta_W} \quad *) \qquad (2.1)$$

where

$$M \equiv M_W = \frac{38}{\sin\Theta_W} \text{ GeV}$$

---

*) This relation is true in the doublet Higgs scheme used by Weinberg and Salam.

The relation between M and M_Z is then

$$M_Z = \frac{M^2}{\sqrt{M^2 - (38)^2}} \text{ GeV} \tag{2.2}$$

Finally

$$\tilde{g}^2 = \frac{\pi \alpha}{2 \sin^2 \theta_W} \tag{2.3}$$

We observe that there is only one free parameter conventionally chosen to be $\sin\theta_W$ or M.

3. - $e^+e^- \to W^-e^+\nu$

In the rest of the paper we are going to estimate the cross-sections for the processes

a) $$e^+e^- \longrightarrow W^-e^+\nu$$

and

b) $$e^+e^- \longrightarrow W^+W^-$$

Process a) which we are going to discuss in this section is interesting for the simple reason that the threshold for it is half of that for process b). Thus if in addition the cross-section for it was sizeable one would regard process a) as a relatively cheap source of W bosons. Let us therefore estimate this cross-section.

In Fig. 1 we present the diagrams which contribute, in the lowest order, to process a) in the framework of the W-S model. Only a few of these diagrams give appreciable contributions to the cross-section. These are first of all the diagrams d) and e) with γ exchange, already discussed by many authors [13]. But if $\sqrt{s} \sim M_Z$ also diagrams b) and c)

with Z^0 in the s channel should give an important contribution due to enhancement through the Z propagator. The remaining diagrams can be estimated to be of order 10^{-41} cm^2 or smaller for $80 \leq \sqrt{s} \leq 180$ GeV and thus negligible.

The diagrams d) and e) were calculated for lower energies by many authors [13] [see, particularly, the first paper of Ref. 13] some time ago with the result that these diagrams give $\sigma \sim 10^{-37} - 10^{-38}$ cm^2. These calculations use, however, couplings which are not of Yang-Mills type. Recently the calculation of diagrams d) and e) has been done [17] in the framework of the W-S model. It turns out that for $M = 62$ GeV these diagrams give cross-sections 8.10^{-38} cm^2 and 5.10^{-37} cm^2 for $\sqrt{s} = 80$ GeV and $\sqrt{s} = 150$ GeV, respectively. Thus as in previous calculations the cross-sections are very small.

What remains to be done is to verify whether diagrams b) and c) could give large cross-sections. To our best knowledge, no estimation of the diagrams in question has been done in the literature. Therefore, we have calculated them exactly. Since the calculation is standard, we present only the result.

Taking the total width $\Gamma(Z^0 \to \text{all})$ to be 1-1.5 GeV as estimated in the quark model, we obtain *) for $M = 62$ GeV and $\sqrt{s} = M_Z = 80$ GeV (i.e., at the peak)

$$\sigma_{peak}(e^+e^- \xrightarrow{Z^0} W^-e^+\nu) = \begin{cases} 5 \cdot 10^{-38} \text{ cm}^2 & , \Gamma = 1 \text{ GeV} \\ 2.2\ 10^{-38} \text{ cm}^2 & , \Gamma = 1.5 \text{ GeV} \end{cases}$$

Thus, the cross-section corresponding to diagrams b) and c) is as small as that coming from the diagrams d) and e). Also total cross-sections (all diagrams included) may be small or even smaller than the diagrams discussed since in any gauge model destructive interference between various diagrams is expected.

---

*) It turns out that diagram b) is dominant mainly due to the suppression of diagram c) through the factor $(\frac{1}{2} - \sin^2\theta)^2$ coming from the combination of the vertices $Z^0e^+e^-$ and $e^-\nu W^-$.

In conclusion, the cross-section for the process $e^+e^- \to e^+W^-\nu$ as estimated in the W-S model is for $80 \leq \sqrt{s} \leq 180$ GeV of order 10^{-37} - 10^{-38} cm^2 or smaller and, consequently, the process in question is not very useful for studying W's. Therefore in the next section, we shall turn to the process $e^+e^- \to W^+W^-$ which, although it has a higher threshold, has a cross-section of order 10^{-35} cm^2 for $130 \leq \sqrt{s} \leq 180$ GeV, and thus is experimentally feasible.

4. - $e^+e^- \to W^+W^-$

In this section, we present explicit expressions for the angular distributions and total cross-section in the W-S model for the process $e^+e^- \to W^+W^-$ which we have obtained by means of the rules of Section 2.

The contributing diagrams are given in Fig. 2 *). The variables of interest are

$$s = (p_1 + p_2)^2 = (k_1 + k_2)^2 ,$$

$$t = Q^2 = (p_2 - k_2)^2 = (k_1 - p_1)^2 ,$$

$$Q^2 = M^2 - \frac{s}{2} + \frac{s}{2}\beta\cos\theta^* \qquad (4.1)$$

where

$$\beta = \sqrt{1 - \frac{4M^2}{s}} \qquad (4.2)$$

and θ^* is c.m.s. scattering angle.

In what follows, we shall denote $\theta^* = \theta$ and

$$\sin^2\theta_W \equiv x \qquad (4.3)$$

---

*) Neglecting lepton masses we eliminate contributions coming from the Higgs scalar.

4.1. - Angular distributions

They are given by

$$\frac{d\sigma}{d\Omega} = \frac{\alpha^2}{32 x^2} \beta \left\{ \frac{1}{s} \right\} \sum_{ij} M_{ij} \equiv \sum_{ij} \frac{d\sigma_{ij}}{d\Omega} \tag{4.4}$$

where M_{ij} denote various contributions. For instance, $M_{\nu\nu}$ stands for the contribution of the diagram 2c, whereas $M_{\nu\gamma}$ denotes the $\nu\gamma$ interference term.

In order to write M_{ij} in a compact form we introduce the following distributions

$$F_1(\theta, s) = 2\left[\frac{s}{M^2}\right] + \frac{\sin^2\theta}{2}\left\{ \left[\frac{s}{Q^2}\right]^2 + \frac{1}{4}\left[\frac{s}{M^2}\right]^2 \right\}\beta^2, \tag{4.5}$$

$$F_2(\theta, s) = \beta^2 \left(16\left[\frac{s}{M^2}\right] + \left\{ \left[\frac{s}{M^2}\right]^2 - 4\left[\frac{s}{M^2}\right] + 12 \right\} \sin^2\theta \right), \tag{4.6}$$

$$F_3(\theta, s) = 16\left(1 + \frac{M^2}{Q^2}\right) + 8\beta^2\left[\frac{s}{M^2}\right] + \beta^2 \frac{\sin^2\theta}{2}\left[\left(\frac{s}{M^2}\right)^2 - 2\left(\frac{s}{M^2}\right) - 4\left(\frac{s}{Q^2}\right) \right]. \tag{4.7}$$

Notice that $F_i(\theta, s)$ are dimensionless.

The M_{ij} contributions are then given as follows

$$M_{\nu\nu} = F_1(\theta, s), \tag{4.8}$$

$$M_{\gamma\gamma} = x^2 F_2(\theta, s), \tag{4.9}$$

$$M_{ZZ} = \left(x^2 - \frac{x}{2} + \frac{1}{8}\right) \frac{s^2}{(s - M_Z^2)^2} F_2(\theta, s), \tag{4.10}$$

$$M_{Z\gamma} = 2x\left(\frac{1}{4} - x\right) \frac{s}{(s - M_Z^2)} F_2(\theta, s), \tag{4.11}$$

$$M_{\nu Z} = \left(x - \frac{1}{2}\right) \frac{s}{(s - M_Z^2)} F_3(\theta, s) \tag{4.12}$$

and

$$M_{\gamma\nu} = - \alpha F_3(\theta, s) \tag{4.13}$$

Thus (4.4)-(4.13) give $(d\sigma/d\Omega)(e^+e^- \to W^+W^-)$ in the W-S model.

Before we go on to present our results for σ_{tot} we would like to make a few comments.

First $M_{\gamma\gamma}$ as given by (4.9) agrees with that of Cabibbo and Gatto [10] calculated 15 years ago. This contribution alone violates unitarity *). Adding other contributions and arranging the couplings in the Yang-Mills way, we restore unitarity. This can be easily checked on the basis of the above equations and will be more evident when we give the asymptotic formula for σ_{tot}.

Second, the distributions $M_{\gamma\gamma}$, M_{ZZ} and $M_{Z\gamma}$, if properly normalized, are the same $[(1/\sigma_{ij})(d\sigma_{ij}/d\Omega)$ are the same$]$. This applies also to $M_{\nu Z}$ and $M_{\nu\gamma}$.

4.2. - Total cross-section

It is given by **)

$$\sigma = \frac{\pi \alpha^2}{8 x^2} \beta \left\{\frac{1}{s}\right\} \sum_{ij} \bar{\sigma}_{ij} \equiv \sum_{ij} \sigma_{ij} \, . \tag{4.14}$$

In order to write $\bar{\sigma}_{ij}$ in a compact form, we introduce the following cross-sections

$$\sigma_1 = 2\left[\frac{s}{M^2}\right] + \frac{1}{12}\left[\frac{s}{M^2}\right]^2 \beta^2 + 4\left\{\left(1 - 2\frac{M^2}{s}\right)\frac{L}{\beta} - 1\right\} , \tag{4.15}$$

$$\sigma_2 = 16\left[\frac{s}{M^2}\right]\beta^2 + \frac{2}{3}\beta^2\left(\left[\frac{s}{M^2}\right]^2 - 4\left[\frac{s}{M^2}\right] + 12\right) , \tag{4.16}$$

---

*) Asymptotically $M_{\gamma\gamma} \sim s^2$ instead of $M_{\gamma\gamma} \sim$ const.

**) Notice that $\bar{\sigma}_{ij} = (1/4\pi)\int d\Omega \, M_{ij}$.

$$\sigma_3 = 16 - 32\left[\frac{M^2}{s}\right]\frac{L}{\beta} + 8\beta^2\left[\frac{s}{M^2}\right] + \beta^2\frac{1}{3}\left[\frac{s}{M^2}\right]^2\left(1-2\frac{M^2}{s}\right) + 4\left(1-2\frac{M^2}{s}\right) - 16\left[\frac{M^2}{s}\right]^2\frac{L}{\beta} \tag{4.17}$$

where

$$L = \ln\left|\frac{1+\beta}{1-\beta}\right| . \tag{4.18}$$

Then

$$\tilde{\sigma}_{\nu\nu} = \sigma_1 , \tag{4.19}$$

$$\tilde{\sigma}_{\gamma\gamma} = x^2\,\sigma_2 , \tag{4.20}$$

$$\tilde{\sigma}_{ZZ} = \left(x^2 - \frac{x}{2} + \frac{1}{8}\right)\frac{s^2}{(s-M_Z^2)^2}\,\sigma_2 , \tag{4.21}$$

$$\tilde{\sigma}_{Z\gamma} = 2\left(\frac{1}{4}-x\right)x\,\frac{s}{(s-M_Z^2)}\,\sigma_2 , \tag{4.22}$$

$$\tilde{\sigma}_{\nu Z} = \left(x-\frac{1}{2}\right)\frac{s}{(s-M_Z^2)}\,\sigma_3 \tag{4.23}$$

and

$$\tilde{\sigma}_{\gamma\nu} = -x\,\sigma_3 \tag{4.24}$$

Thus (4.14)-(4.24) give $\sigma(e^+e^-\to W^-W^+)$ in the W-S model.

We can check our results for the total cross-section by comparing them to those obtained by Sushkov, Flambaum and Khriplovich [11]. These authors give only $\sigma(e^+e^-\to W^+W^-)$ with all contributions added up. When we sum up all the contributions (4.20)-(4.24) and introduce the variable

$$y \equiv \frac{s}{M^2} \tag{4.25}$$

we obtain the result of Ref. 13)

$$\sigma = \frac{\pi\alpha^2\beta}{2x^2 s}\left\{\left(1+\frac{2}{y}+\frac{2}{y^2}\right)\frac{L}{\beta} - \frac{5}{4}\right.$$

$$+ \frac{M_Z^2(1-2x)}{(s-M_Z^2)}\left[\frac{2}{y^2}(1+2y)\frac{L}{\beta} - \frac{y}{12} - \frac{5}{3} - \frac{1}{y}\right]$$

$$\left. + \frac{M_Z^4(8x^2-4x+1)\beta^2}{48(s-M_Z^2)^2}(y^2+20y+12)\right\}. \qquad (4.26)$$

4.3. - Asymptotic behaviour

Although each of the cross-sections, as given by (4.14)-(4.24), grows as s at $s\to\infty$ and violates unitarity the sum of all contributions behaves properly. This is the standard result of Yang-Mills "theories" [2),15)].

We obtain, as $s\to\infty$,

$$\sigma = \frac{\pi\alpha^2}{96x^2}\frac{1}{s}\left\{48\ln\frac{s}{M^2} + \left(\frac{M_Z}{M}\right)^4(8x^2-4x+1)\right.$$

$$\left. + \left(\frac{M_Z}{M}\right)^2(8x-4) - 60\right\}$$

$$= \frac{\pi\alpha^2}{96x^2}\frac{1}{s}\left\{48\ln\frac{s}{M^2} + \frac{8x-3}{(1-x)^2} - 60\right\}$$

$$\underset{s\to\infty}{\Rightarrow} \quad \frac{\pi\alpha^2}{2x^2}\frac{1}{s}\ln\frac{s}{M^2}\,. \qquad (4.27)$$

The $\ell n(s/M^2)$ term comes from the neutrino diagram.

4.4. - Numerical results

The only free parameter in the Weinberg-Salam model is the mass of the W boson, which, however, must be larger than 38 GeV. From the application of W-S model to other processes, one expects $50 \leq M \leq 70$ GeV ($0.25 \leq \sin^2\theta_W \leq 0.55$), the canonical value being $M = 62$ GeV ($\sin^2\theta_W = 3/8$). Notice that for this range of values of M, $76 \leq M_Z \leq 84$ GeV and consequently the enhancement through the Z propagator is very weak since M_Z is much smaller than the threshold for the process in question. Equation (2.2) tells us that a strong enhancement would be possible if $M \leq 45$ GeV or $\sin^2\theta_W \geq 0.75$, a rather unrealistic value. In what follows, most of our results are presented for $M = 50$, 62 and 70 GeV.

4.4.1. - Total cross-sections

In Fig. 4, we have plotted $\sigma(e^+e^- \to W^+W^-)$ as a function of $\sqrt{s}$. We observe the increase of the cross-section after the threshold and a $\sim 1/s$ decrease at larger values of s. For all three values of M considered $\sigma \sim 10^{-8}$ mb $\approx 10^{-35}$ cm^2 at its maximum value. There is a 40% rise in the cross-section (at its maximal value) when we increase M from 50 to 70 GeV.

In Fig. 5, we have plotted the contributions from various diagrams as well as from interference terms as a function of $\sqrt{s}$ for $M = 62$ GeV. We observe that in the range of s considered $\sigma_{\nu\nu} > \sigma_{\gamma\gamma} > \sigma_{ZZ}$ and all interference terms are negative and large indicating strong cancellations between various diagrams. This is more clearly seen in the Table where we have collected numerical values for various contributions. Observe that already at $\sqrt{s} = 300$ GeV $\sigma/\tilde{\sigma} \approx 0.15$ implying that the Z^0 is important in the cancellations in question. Obviously the effect becomes more and more pronounced as s is increased.

4.4.2. - Angular distributions

In Fig. 6, we present the normalized angular distributions $\frac{1}{\sigma}(d\sigma/d\cos\theta)$ at various $\sqrt{s}$ for the value $M = 62$ GeV. One observes strong asymmetry in $\cos\theta$. The distribution is strongly peaked at $\cos\theta \approx 1$ and this effect is more pronounced at higher energies. If we look at Eq. (4.5) we see that this peaking of $d\sigma/d\cos\theta$ comes from the ν exchange diagram.

Figure 7 represents $1/\sigma(d\sigma/d\cos\theta)$ at $\sqrt{s} = 160$ GeV for various values of M. As might be expected, the effect of increasing M at fixed s is to make the distribution flatter.

Finally in Fig. 8 we have presented for completeness the angular distributions corresponding to various contributing diagrams and their interference terms. The large differences between distributions in Fig. 8 and the total distribution in Fig. 7 indicate again strong cancellations.

5. - SUMMARY

In this paper we have presented explicit formulae (see Section 4) and corresponding numerical estimates of the total cross-sections and angular distributions for the process $e^+e^- \to W^+W^-$ in the framework of the W-S model. We have also estimated the contribution of Z^o to the process $e^+e^- \to e^+W^-\nu$ (other contributions have been calculated by other authors [13),17)]).

Our principal findings are the following.

A) The cross-section for the process $e^+e^- \to e^+W^-\nu$ is, for $80 \leq \sqrt{s} \leq 150$ GeV, of the order $10^{-37} - 10^{-38}$ cm^2 and thus is very difficult to measure.

B) The cross-section for the process $e^+e^- \to W^+W^-$ is of order 10^{-35} cm^2 for $130 \leq \sqrt{s} \leq 180$ GeV and $50 \leq M_W \leq 70$ GeV and thus large enough to be measured.

C) The angular distributions for $e^+e^- \to W^+W^-$ are very asymmetric being very strongly peaked forward. This asymmetry increases with energy. For fixed s increasing M_W makes the distribution flatter.

D) There are very strong cancellations between various diagrams contributing to $e^+e^- \to W^+W^-$ already at energies just above threshold, implying that in any calculation all diagrams should be included. This is seen both in total cross-sections (see the Table) as well as in angular distributions.

These results suggest that it would be useful to have e^+e^- machines in the energy range $120 \leq \sqrt{s} \leq 180$ GeV. Not only is the W production cross-section optimal in this energy range, but also the structure of gauge theories, in particular the strong cancellations could be tested.

ACKNOWLEDGEMENTS

We are grateful to John Ellis, Mary K. Gaillard and Jacques Prentki for many suggestions and discussions. Particular thanks are due to John Ellis and Mary K. Gaillard for reading the manuscript.

We also thank Frederik Berends and Gerbrand Komen for informing us about Refs. 11)-13).

$\sqrt{s}$ (GeV)	σ	$\sigma_{\gamma\gamma}$	$\sigma_{\nu\nu}$	σ_{ZZ}	$\sigma_{\nu Z}$	$\sigma_{Z\gamma}$	$\sigma_{\gamma\nu}$	$\tilde{\sigma}$
130	0.81	0.10	0.97	0.14	-0.10	-0.11	-0.19	0.88
150	1.13	0.70	2.11	0.74	-0.54	-0.65	-1.22	1.59
200	0.93	2.16	3.52	1.67	-1.33	-1.70	-3.39	2.29
300	0.57	4.69	5.44	3.00	-2.41	-3.37	-6.78	3.35

Numerical values for the various contributions to $\sigma(e^+e^- \to W^+W^-)$ (10^{-8} mb) for $M = 62$ GeV and $\sqrt{s} = 130$, 150, 200 and 300 GeV.
$\tilde{\sigma} = \sigma_{\gamma\gamma} + \sigma_{\nu\nu} + \sigma_{\gamma\nu}$ is the cross-section without Z^0 contribution.

REFERENCES

1) S. Weinberg - Phys.Rev.Letters 19, 1264 (1967) ; 27, 1688 (1971) ;
A. Salam - in Elementary Particle Physics (ed. N. Svartholm, Almqvist and Wiksells, Stockholm, 1968), p. 367.

2) See, for instance :
E.S. Abers and B.W. Lee - Physics Reports 9C, 1 (1973) ;
C.H. Llewellyn Smith - in Scottish Universities Summer School 1973 London, Academic Press (1974).

3) S. Glashow, J. Iliopoulos and L. Maiani - Phys.Rev. D2, 1285 (1970).

4) For a review, see :
D.C. Cundy - London Conference (1974), p. 131.

5) J.J. Aubert et al. - Phys.Rev.Letters 33, 1404 (1974) ;
J.E. Augustin et al. - Phys.Rev.Letters 33, 1406 (1974) ;
C. Bacci et al. - Phys.Rev.Letters 33, 1408 (1974) ;
For a recent review, see, for instance :
B. Richter - SLAC-PUB-1737 (April 1976).

6) G. Goldhaber et al. - Phys.Rev.Letters 37, 255 (1976) ;
I. Peruzzi et al. - SLAC-PUB 1776 (1976).

7) M.L. Perl et al. - Phys.Rev.Letters 35, 1489 (1975) ;
M. Cavalli-Sforza et al. - Phys.Rev.Letters 36, 558 (1976) ;
M.L. Perl - SLAC-PUB-1748 (1976).

8) J. Ellis, M.K. Gaillard and D.V. Nanopoulos - Nuclear Phys. B106, 292 (1976).

9) R.W. Brown and J. Smith - Phys.Rev. D3, 207 (1971) ;
R.W. Brown, R.H. Hobbs and J. Smith - Phys.Rev. D4, 794 (1971) ;
C.H. Llewellyn Smith - Physics Reports 3C, 261 (1972), and references therein ;
R.L. Jaffe and J.R. Primack - Nuclear Phys. B61, 317 (1973) ;
J. Finjord - Nordita Preprint 76/22 (1976) ;
R. Petronzio - Istituto di Fisica G. Marconi Preprint (1976) ;
See also first paper of Ref. 13).

10) N. Cabibbo and R. Gatto - Phys.Rev. 124, 1577 (1961) ;
Y.S. Tsai and A.C. Hearn - Phys.Rev. 140, 721 (1965).

11) O.P. Sushkov, V.V. Flambaum and I.B. Khriplovich - Soviet J.Nucl.Phys. 20, 537 (1975).

12) G. Komen - Nuclear Phys. B84, 323 (1975).

13) F.A. Berends and G.B. West - Phys.Rev. D1, 122 (1970) ;
E.A. Choban - Soviet J.Nucl.Phys. 13, 354 (1971) ;
A.M. Altukhov and I.B. Khriplovich - Soviet J.Nucl.Phys. 13, 359 (1971) ;
M. Hayashi - Acta Physica Polonica B5, 97 (1974) ;
R.W. Brown and J. Smith - Phys.Rev. D3, 207 (1971).

14) J.C. Pati and A. Salam - Phis.Rev. D8, 1240 (1973) ;
H. Georgi and S.L. Glashow - Phys.Rev.Letters 32, 438 (1974) ;
H. Fritzsch and P. Minkowski - Ann.Phys. 93, 222 (1975).

15) C.H. Llewellyn Smith - Phys.Letters 46B, 233 (1973) ;
J.M. Cornwall, D.N. Levin and G. Tiktopoulos - Phys.Rev.Letters 30, 1268 (1973).

16) K.F. Fujikawa, B.W. Lee and A.I. Sanda - Phys.Rev. D6, 2923 (1972).

17) J. Prentki and G. Preparata - Private communication.

FIGURE CAPTIONS

Figure 1 Diagrams contributing in the lowest order to the process $e^+e^- \to W^-e^+\nu$.

Figure 2 Diagrams contributing in the lowest order to the process $e^+e^- \to W^+W^-$.

Figure 3 Feynman rules in the Weinberg-Salam model in the unitary gauge (Relations between various couplings are in Section 2).

Figure 4 $\sigma(e^+e^- \to W^-W^+)$ in the Weinberg-Salam model as a function of $\sqrt{s}$ for $M = 50$, 62 and 70 GeV.

Figure 5 Contributions to $\sigma(e^+e^- \to W^-W^+)$ from various diagrams as functions of $\sqrt{s}$ for $M = 62$ GeV.

Figure 6 Angular distributions $1/\sigma\ (d\sigma/d\cos\theta)$ for the process $e^+e^- \to W^-W^+$ for $M = 62$ GeV and $\sqrt{s} = 130$, 160, 200 GeV in the Weinberg-Salam model.

Figure 7 Angular distributions $1/\sigma\ (d\sigma/d\cos\theta)$ for the process $e^+e^- \to W^-W^+$ for $\sqrt{s} = 160$ GeV and $M = 50$, 62, 70 GeV.

Figure 8 Contributions to $1/\sigma\ (d\sigma/d\cos\theta)\ (e^+e^- \to W^-W^+)$ from various diagrams for $M = 62$ GeV and $\sqrt{s} = 130$, 160, 200 GeV.

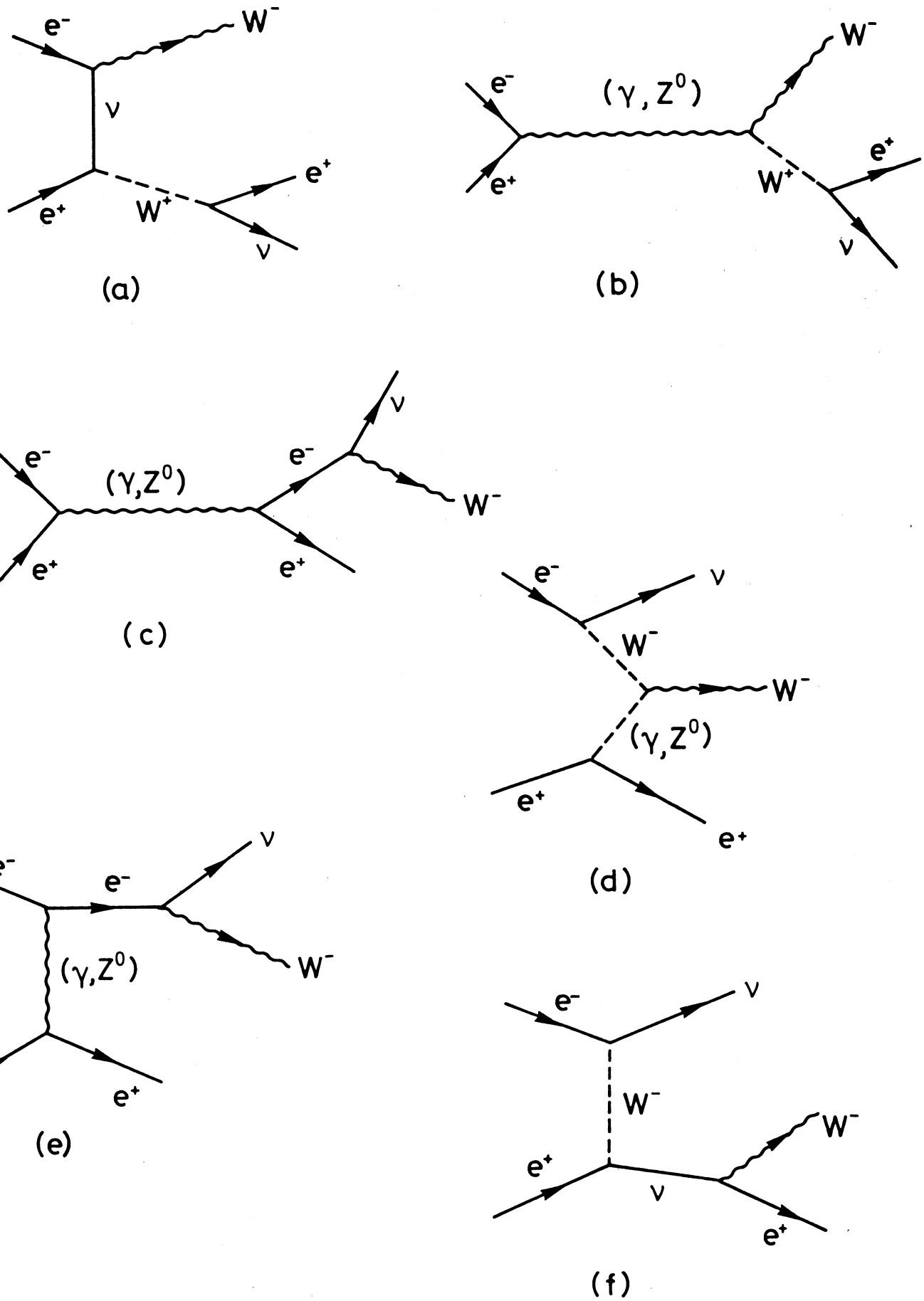
e⁻
W⁻
ν
e⁺
W⁺
e⁺
ν
(a)
(γ, Z⁰)
W⁻
e⁻
e⁺
e⁺
W⁺
ν
(b)
ν
e⁻
(γ,Z⁰)
e⁻
W⁻
e⁺
e⁺
(c)
e⁻
ν
W⁻
W⁻
(γ,Z⁰)
e⁺
e⁺
(d)
ν
e⁻
e⁻
(γ,Z⁰)
W⁻
e⁺
e⁺
(e)
e⁻
ν
W⁻
W⁻
e⁺
ν
e⁺
(f)

FIG.1

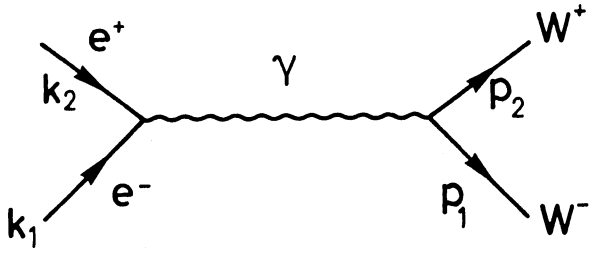

(a)

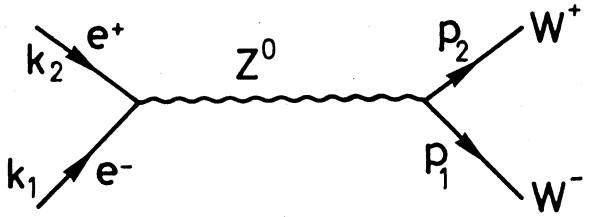

(b)

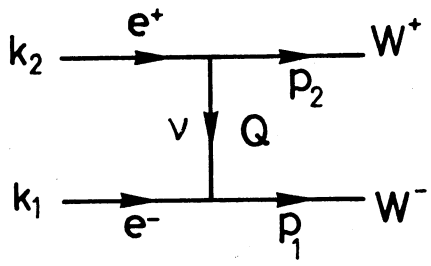

(c)

FIG. 2

$A \equiv \gamma$: 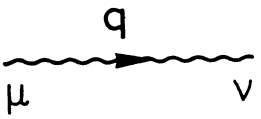

$$-i\,\frac{g_{\mu\nu}}{q^2}$$

$Z^0, W^{\pm}$: 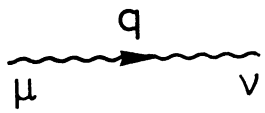

$$-i\left[g_{\mu\nu}-\frac{q_\mu\, q_\nu}{M^2}\right]\Big/\left[q^2-M^2\right]$$

$\nu, e^{\pm}$: 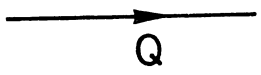

$$\frac{i\,\not{Q}}{Q^2}$$

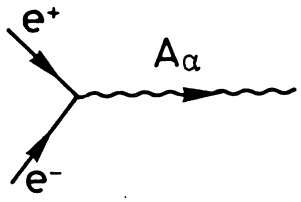

$$-ie\,\gamma_\alpha$$

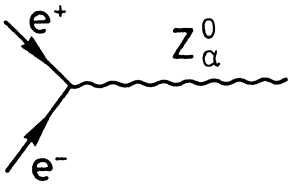

$$i\,G\left[a+b\,\gamma_5\right]\gamma_\alpha$$

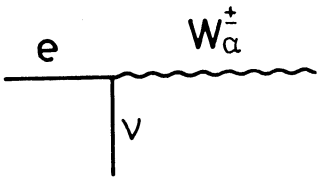

$$-i\,\tilde{g}\,\gamma_\alpha(1-\gamma_5)$$

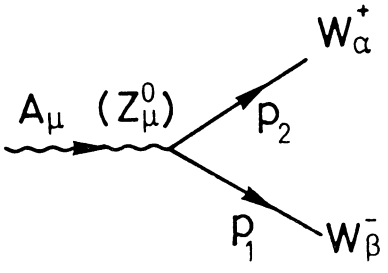

$$i\begin{pmatrix} e \\ Z \end{pmatrix}\Big\{ g_{\alpha\beta}(p_1-p_2)_\mu + p_{2\beta}\, g_{\mu\alpha} - p_{1\alpha}\, g_{\mu\beta} + g_{\alpha\mu}(p_1+p_2)_\beta - g_{\beta\mu}(p_1+p_2)_\alpha \Big\}$$

FIG. 3

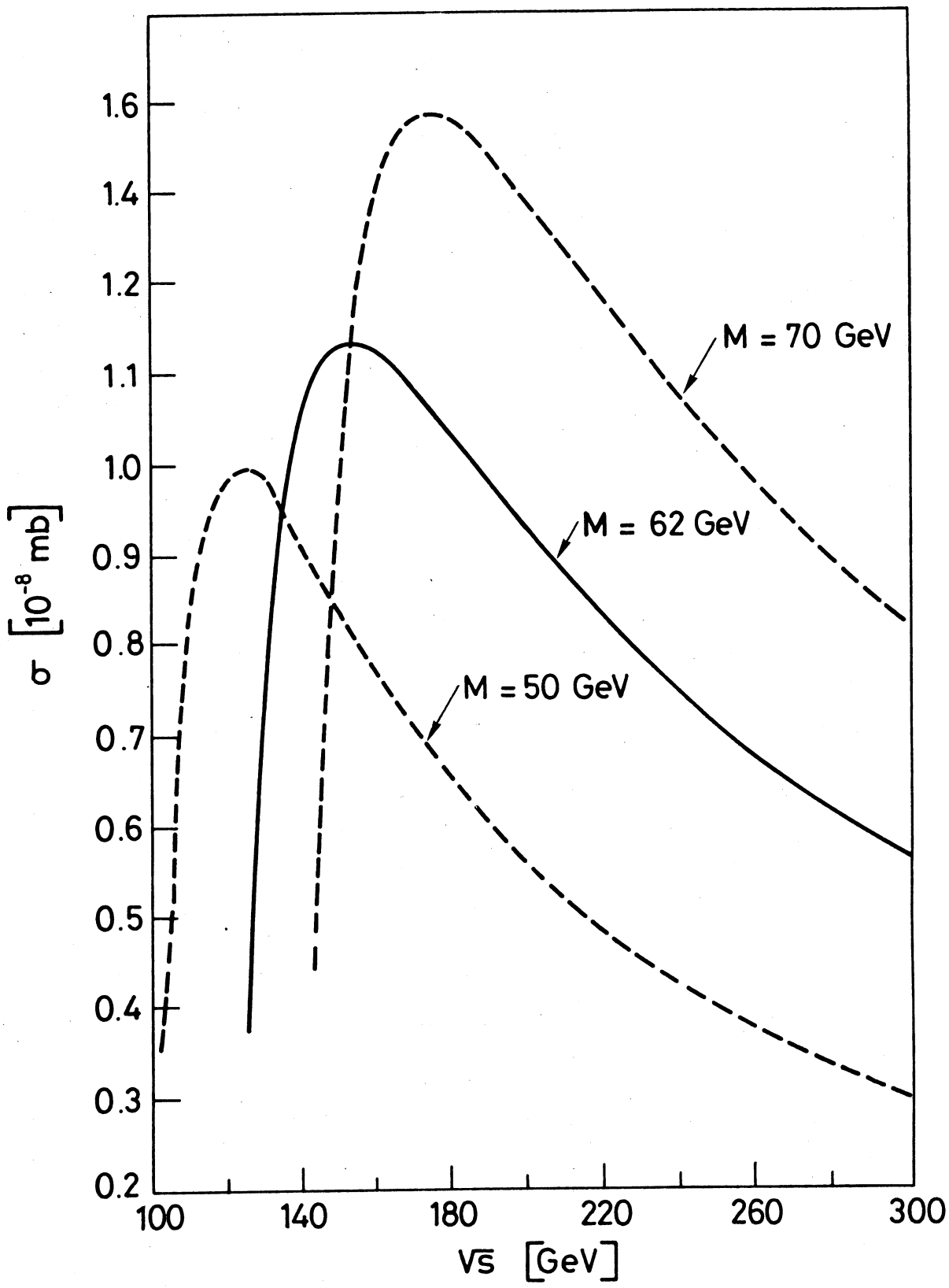
1.6
1.4
1.2
1.1
1.0
0.9
0.8
0.7
0.6
0.5
0.4
0.3
0.2
b [10⁻⁸ mb]
M = 70 GeV
M = 62 GeV
M = 50 GeV
100
140
180
220
260
300
√s [GeV]

FIG. 4

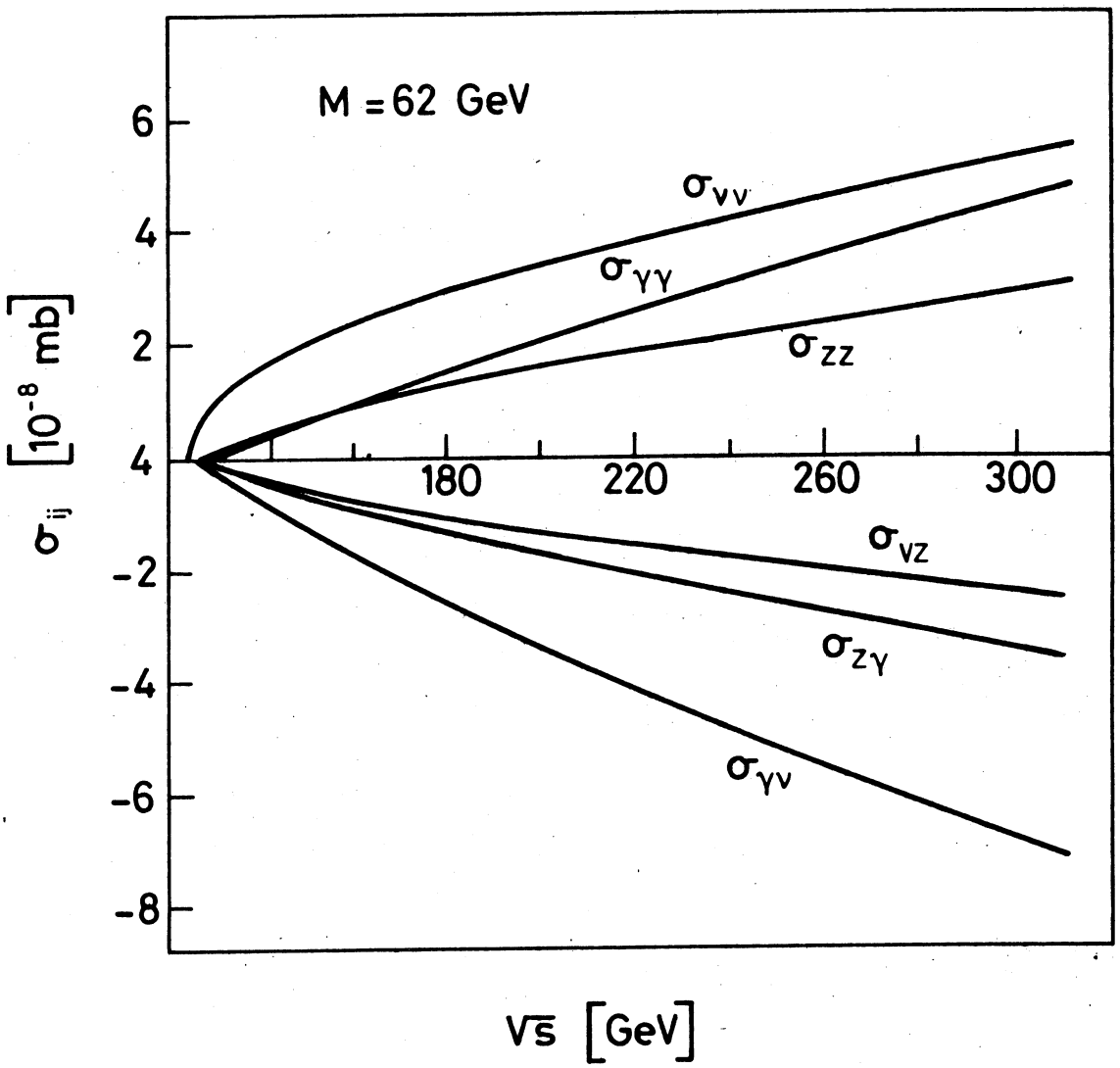
M = 62 GeV
6
4
2
4
-2
-4
-6
-8
180
220
260
300
$\sigma_{\nu\nu}$
$\sigma_{\gamma\gamma}$
σ_{zz}
$\sigma_{\nu z}$
$\sigma_{z\gamma}$
$\sigma_{\gamma\nu}$
σ_{ij} [10^{-8} mb]
$\sqrt{s}$ [GeV]

FIG. 5

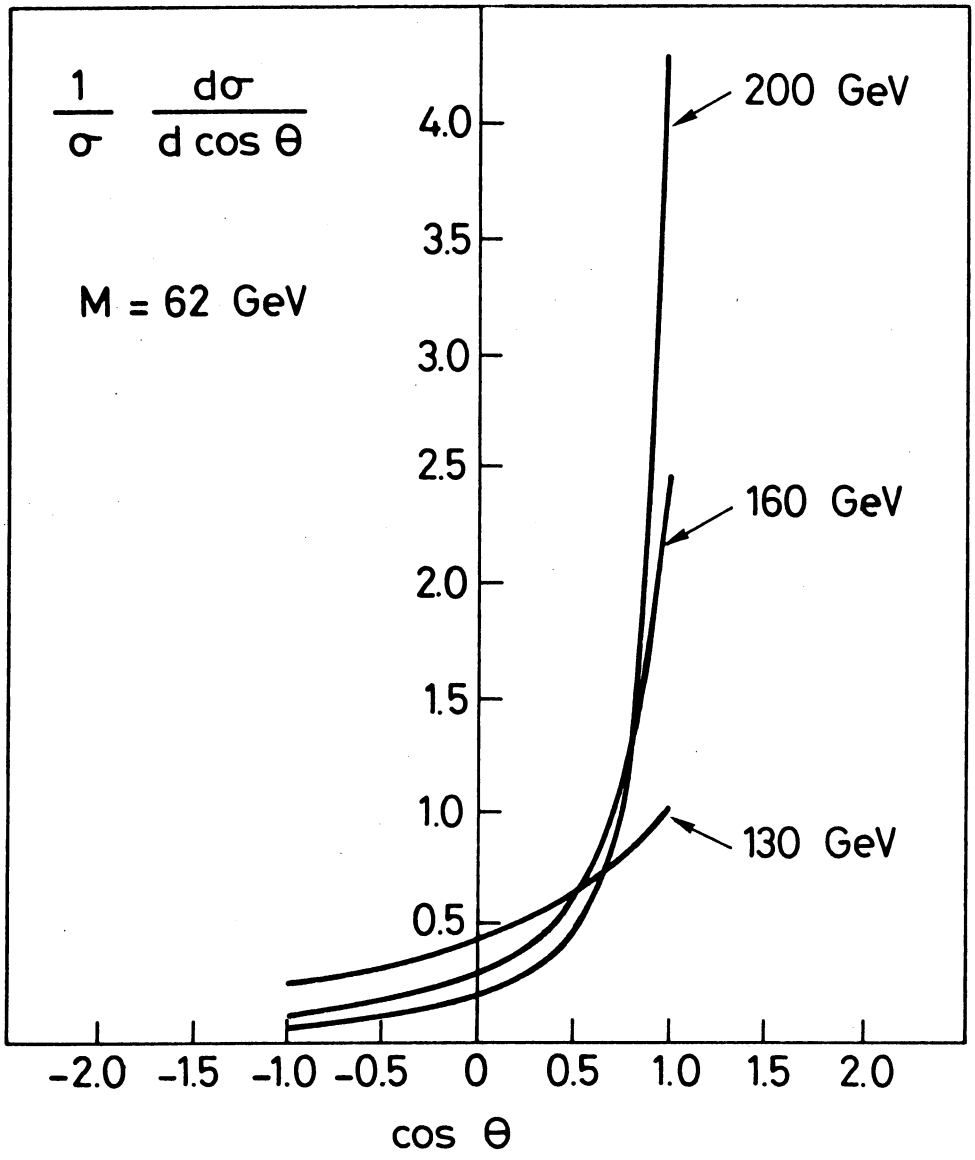
1/σ dσ/d cos θ
M = 62 GeV
200 GeV
160 GeV
130 GeV
4.0
3.5
3.0
2.5
2.0
1.5
1.0
0.5
-2.0
-1.5
-1.0
-0.5
0
0.5
1.0
1.5
2.0
cos θ

FIG. 6

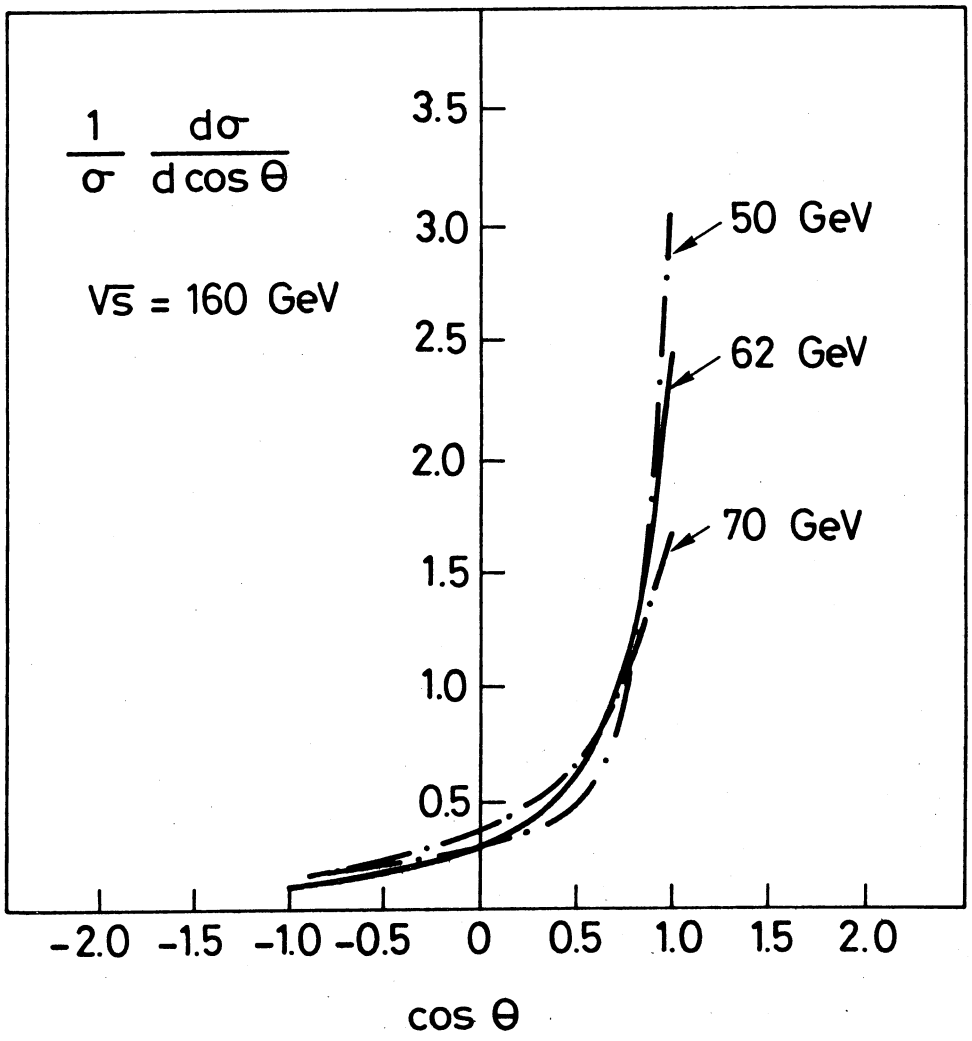
$\frac{1}{\sigma}\frac{d\sigma}{d\cos\theta}$
$\sqrt{s}$ = 160 GeV
50 GeV
62 GeV
70 GeV
3.5
3.0
2.5
2.0
1.5
1.0
0.5
-2.0 -1.5 -1.0 -0.5 0 0.5 1.0 1.5 2.0
cos θ

FIG. 7

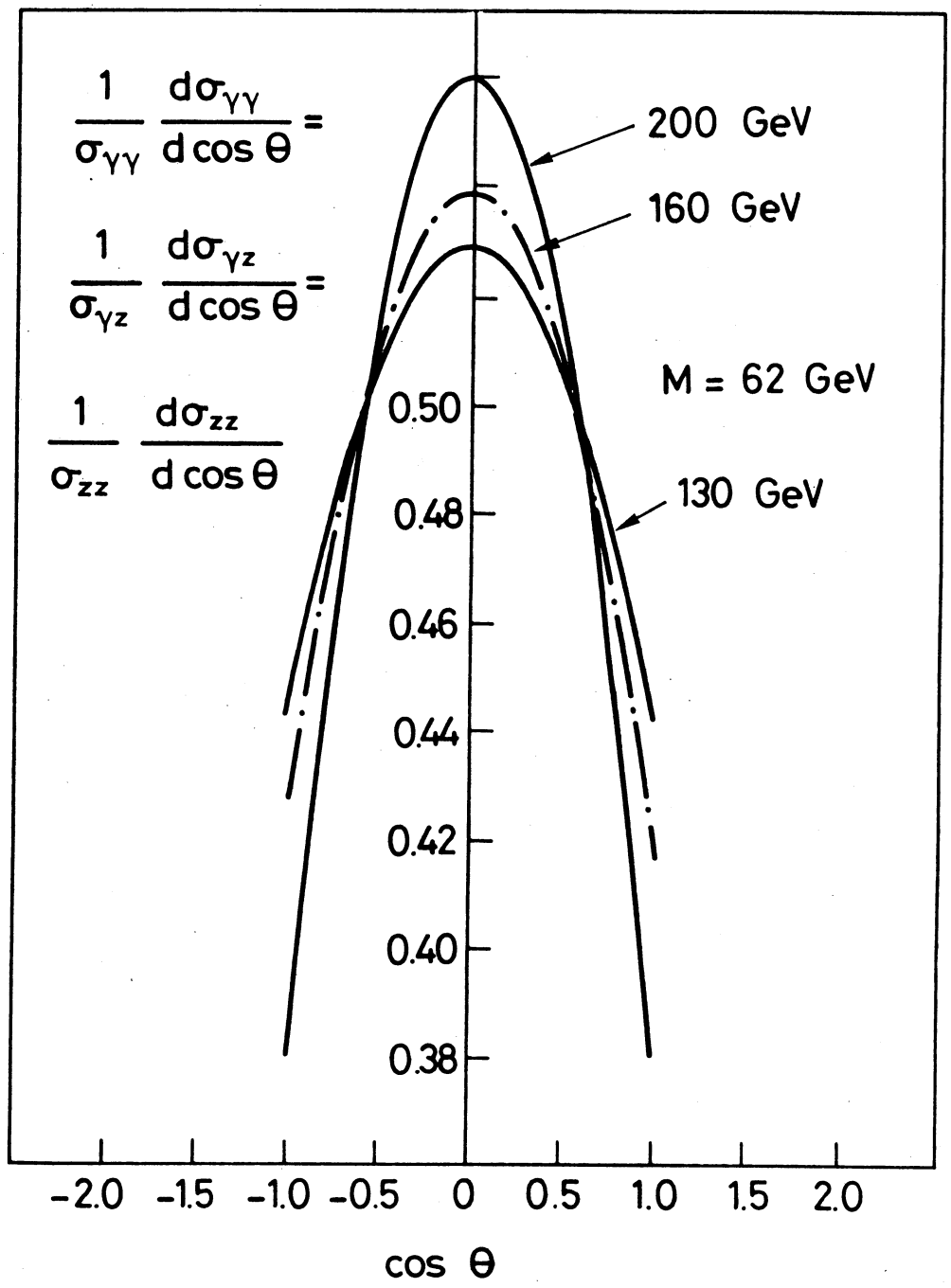
$\frac{1}{\sigma_{\gamma\gamma}} \frac{d\sigma_{\gamma\gamma}}{d\cos\theta} =$
$\frac{1}{\sigma_{\gamma z}} \frac{d\sigma_{\gamma z}}{d\cos\theta} =$
$\frac{1}{\sigma_{zz}} \frac{d\sigma_{zz}}{d\cos\theta}$
200 GeV
160 GeV
M = 62 GeV
130 GeV
0.50
0.48
0.46
0.44
0.42
0.40
0.38
-2.0 -1.5 -1.0 -0.5 0 0.5 1.0 1.5 2.0
cos θ

FIG. 8 a

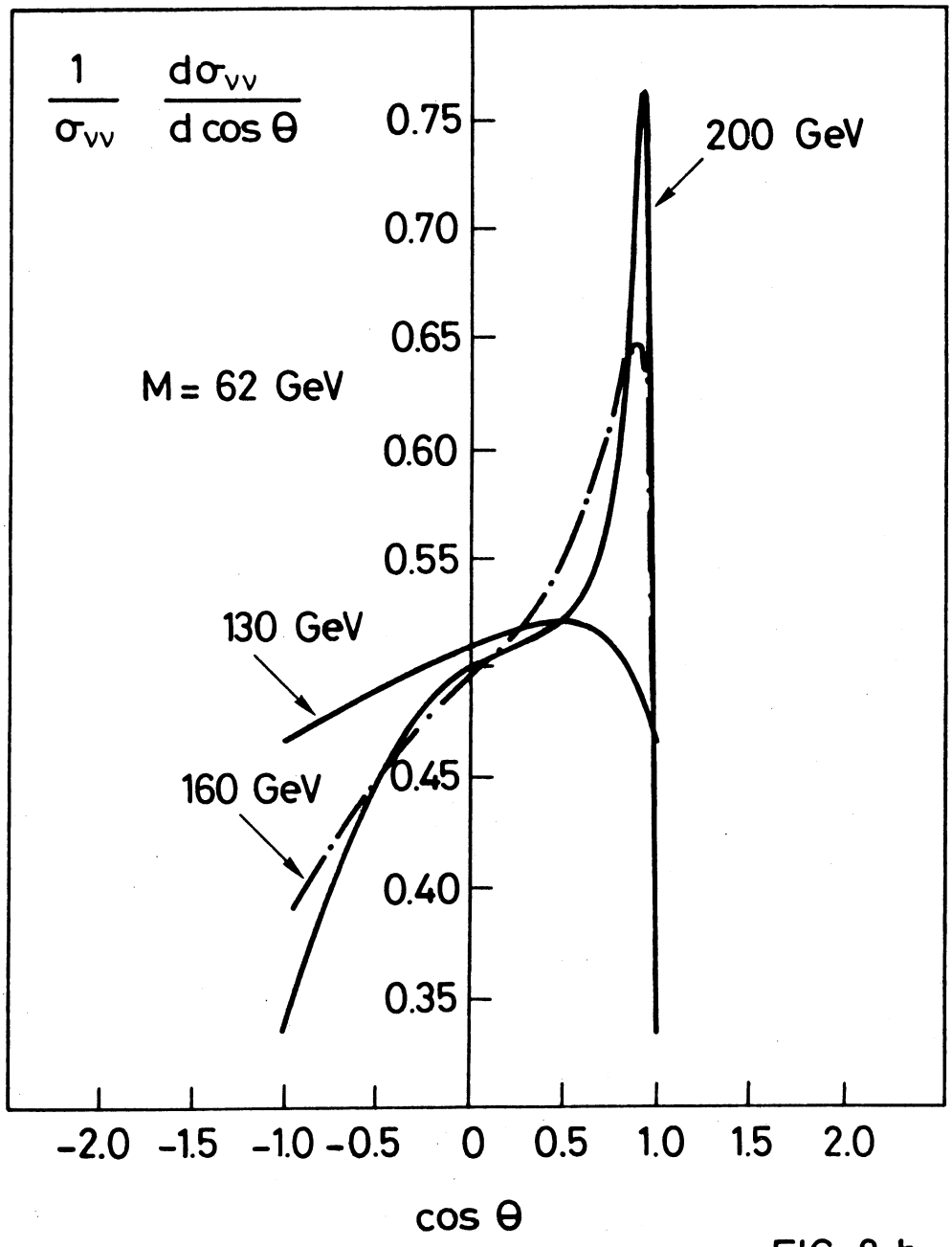
$\frac{1}{\sigma_{\nu\nu}} \frac{d\sigma_{\nu\nu}}{d\cos\theta}$
0.75
0.70
0.65
0.60
0.55
0.45
0.40
0.35
200 GeV
M = 62 GeV
130 GeV
160 GeV
-2.0 -1.5 -1.0 -0.5 0 0.5 1.0 1.5 2.0
cos θ

FIG. 8 b

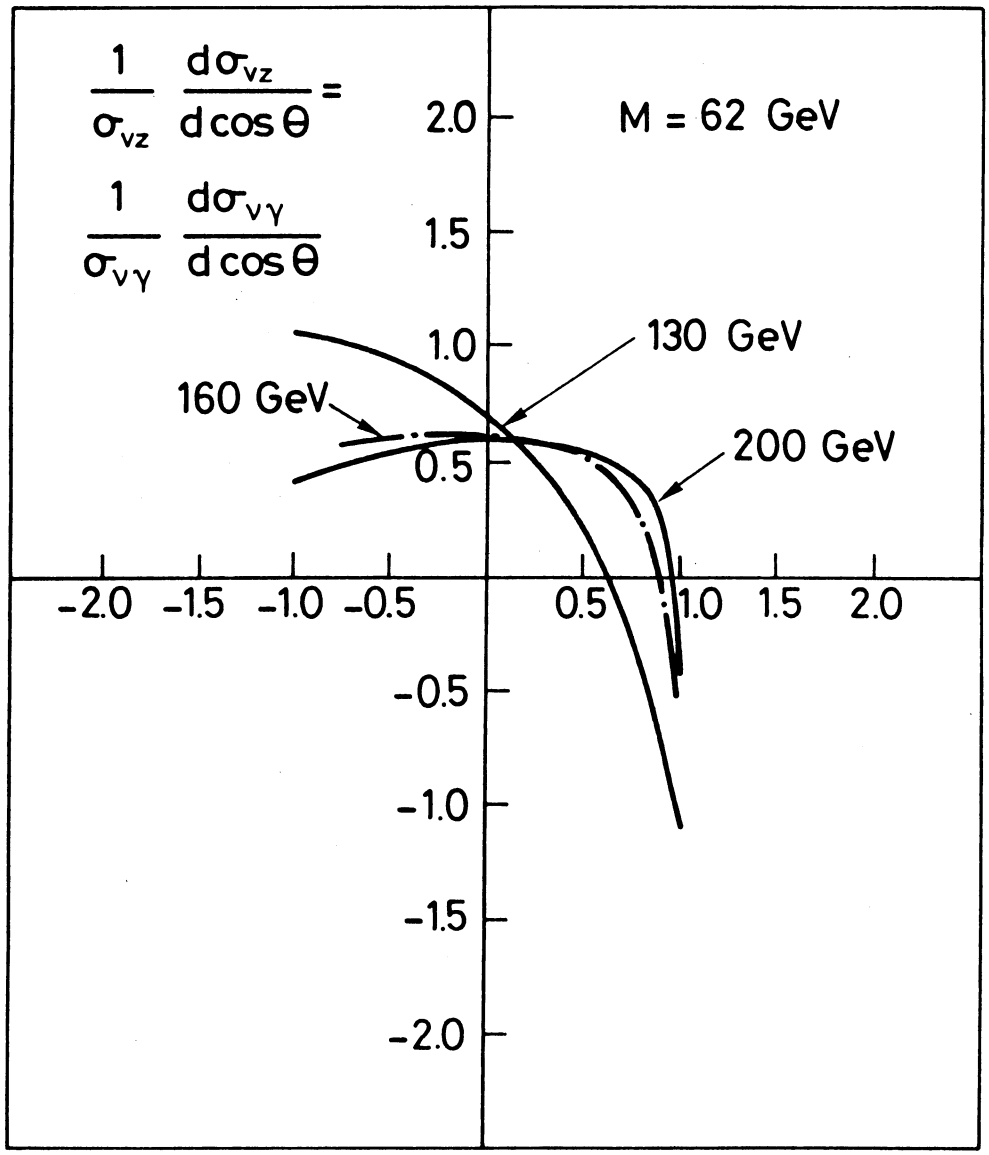
$\frac{1}{\sigma_{\nu z}} \frac{d\sigma_{\nu z}}{d\cos\theta} =$
$\frac{1}{\sigma_{\nu\gamma}} \frac{d\sigma_{\nu\gamma}}{d\cos\theta}$
M = 62 GeV
130 GeV
160 GeV
200 GeV
2.0
1.5
1.0
0.5
-0.5
-1.0
-1.5
-2.0
-2.0 -1.5 -1.0 -0.5
0.5 1.0 1.5 2.0
cos θ

FIG. 8 c